Northumbria University
NEWCASTLE

University**Library**

Applied Thermal Engineering 179 (2020) 115629

Contents lists available at ScienceDirect

Applied Thermal Engineering

journal homepage: www.elsevier.com/locate/apthermeng

A greener seawater desalination method by direct-contact spray evaporation and condensation (DCSEC): Experiments

Raid Alrowais[a,b], Chen Qian[a], Muhammad Burhan[a], Doskhan Ybyraiymkul[a], Muhammad Wakil Shahzad[c], Kim Choon Ng[c,*]

[a] Water Desalination and Reuse Center (WDRC), King Abdullah University of Science and Technology, Thuwal 23955-690096, Saudi Arabia
[b] Civil Engineering Department, AlJouf University, Skaka, Saudi Arabia
[c] Mechanical & Construction Engineering Department, Northumbria University, Newcastle Upon Tyne, UK

HIGHLIGHTS

- A greener seawater desalination method for sustainable future.
- Simple hollow vessel design, no heat transfer interfaces, exploits liquid flashing.
- Robust operation, lowest CAPEX and OPEX amongst all practical desalination methods.
- Resilient to high salinity, feed temperature with micro-bubble enhanced flashing.

ARTICLE INFO

Keywords:
Thermally-driven seawater desalination
Direct spray evaporator and condenser design
Multi-stage
Micro-vapor-bubble enhancement

ABSTRACT

Owing to the high specific energy consumption of conventional seawater desalination methods available hitherto, there is much motivation for designing greener desalination processes. As a greener desalination process, it should consume lower top-brine temperatures for the seawater feed as well as minimum chemical use for brine treatment. In this paper, a direct-contact spray-assisted evaporation and condensation (DCSEC) is presented that addresses the above-mentioned requirements of greener desalination. We have tested both the single-stage and multi-stage configurations of DCSEC process with seawater (3.5% by weight salinity) from Red Sea. The performance of the system was investigated for a feed flow rate of 6 L/minute when the evaporator chamber temperature was varied from 38 °C to 60 °C. From the experiments, maximum distillate production of 31 L/hr m^3 was recorded at 60 °C feed temperature for a single-stage configuration. To further enhance the distillate production of DCSEC, an innovative micro/nano-bubbles (M/NBs) generator device is incorporated in the feed supply system which resulted in 34% increase in potable water production at the corresponding inlet feed temperatures.

1. Introduction

In the harsh hot and arid climate, the Gulf Co-operation Council (GCC) countries suffer from an acute scarcity in potable water availability. The daily average water availability per capita in these countries has fallen drastically, below the UN defined acute water stress (AWS) level of 250 m^3, as shown in Table 1 [1,2]. Such a water shortage scenario in GCC is attributed to the dry arid and desert climate, and the dire situation is further compounded by man-made factors, namely the exponential increase in population and the quest for rapid economic growth in the economies. Confronted by these challenges within the desalination industry over the short and near term, the most viable and sustainable solution for solving the demand-supply water gap of the region is by seawater desalination.

Hitherto, there are two major types of seawater desalination systems, namely, the thermally-driven systems such as the multi-stage flashing (MSF), the multi-effect distillation (MED), etc., and the other is work-driven membrane-based desalination system, commonly known as seawater reverse osmosis (SWRO). Due to the severe seawater feed conditions such as the high salinity, silt content (perturbility), and the frequent harmful algae blooms (HABs) [3], an appropriate desalination method must be sought to meet these challenges. In 2008 and 2013, for example, the southern Gulf seawater was hit by severe HABS for a period up to 6 weeks [4,5], and most of the SWRO plants in Oman and

* Corresponding author.
E-mail address: kimchoon.ng@kaust.edu.sa (K.C. Ng).

https://doi.org/10.1016/j.applthermaleng.2020.115629
Received 11 February 2020; Received in revised form 14 June 2020; Accepted 17 June 2020
Available online 29 June 2020

Table 1
The projected water availability per capita in GCC countries from 2010 to 2035.

Country in GCC (Gulf)	Population (Thousands) 2010	Per capita water availability per year by 2010 (m^3/cap).	Projected Population (Thousands) 2035	Per capita water availability per year by 2035 (m^3/cap).
Kuwait	*2,737*	*7.3*	*4,328*	*4.6 ± 1*
UAE	*7,512*	*20.0*	*11,042*	*13.6 ± 2.0*
Qatar	*1,759*	*33.0*	*2,451*	*21.6 ± 2.0*
KSA	*27,448*	*87.4*	*40,444*	*59.3 ± 2.0*
Bahrain	*1,262*	*91.9*	*1,711*	*67.8 ± 3.0*
Oman	*2,803*	*503*	*4,922*	*300 ± 10*

Sharjah (UAE) were forced to stop operating due to the presence of highly toxic algae spices such as the Cyanobacteria and Saxitoxins that are 500 times more toxic than Cyanide [6,7]. As the size of algae spices is of a similar order of magnitude as the pores of SWRO membranes, the likelihood of toxic algae spices polluting the permeate water is high [8]. On the other hand, the evaporative process of heat-driven methods generates water vapor molecules at 2.75 Angstroms diameters. Hence, the 2–10 μm-sized molecules of algae would remain in the solution and gravimetrically filtered. The operation of thermally-driven plants is unaffected throughout the HAB events without any fear of health hazards.

Another important aspect of seawater desalination plants is the unit cost of desalinated water. It comprises both the initial capital or CAPEX (usually defined by \$/m^3 of daily water production) and the annual operation (include electricity or steam, pre- and post-treatment, etc.) costs or OPEX. Table 2 depicts the unit cost of water for the above-mentioned practical desalination, as reported by Global Water Intelligence (GWI, 2018) reports [3,9,10]. Two salient points can be observed from the table: Firstly, the SWRO method has slightly lower capital cost than the thermally-driven methods but the operating cost of the latter is much lower as compared with SWRO due to the higher contribution by electricity. Currently, all existing desalination methods have their CAPEX greater than \$1000/m^3 day of designed capacity, and this is attributed to the costly internal components such as the membranes or the tube heat exchangers within the enclosures. Thus, one of the motivations for the sustainable desalination method is to lower both the CAPEC and OPEX.

The direct-contact spray-assisted evaporation and condensation (DCSEC) methodology has the potential to mitigate the operational issues faced by the existing desalination systems [11]. Being tubeless in the vessels, the direct spray of externally heated seawater (typically up to 65 °C at the top-brine stage) has two distinct advantages: Firstly, initial design cost of the evaporator and condenser vessels are greatly reduced, typically in terms of unit cubic meter of distillate per day, its CAPEX can be less than US\$700/m^3 day. Secondly, the spray of brine into an empty chamber of each stage can mitigate the scale formation as there are virtually no dry spots within the chambers. Consequently, the direct depressurization of the liquid brine in the nozzles resulted in the formation of liquid droplets. The corresponding excess water enthalpy held by the droplets, as they emerged from the nozzles would result in the "vapor flashing" phenomenon, i.e., water vapor evaporates from the surfaces of liquid droplets, reducing its diameter as the droplets traveled down the trajectory paths. The generated vapor in the evaporators then migrates across to the adjacent condenser chambers. Being set at a few degrees lower in vapor temperature within each evaporator to condenser pair, the favorable temperature gradient, the vapor condenses onto the cooler surfaces of distillate or potable water droplets which is drawn from the subsequent lower stages.

Table 2
A comparison of life-cycle unit water cost (US \$/m^3) for various desalination methods [3]

	MSF[a]	MED[b]	SWRO[c]
Thermal	*0.310*	*0.310*	*0.000*
Parts	*0.010*	*0.010*	*0.030*
Chemicals	*0.050*	*0.080*	*0.070*
Labour	*0.080*	*0.080*	*0.100*
Membranes	*0.000*	*0.000*	*0.030*
Electrical	*0.600*	*0.420*	*0.720*
Capital cost	*0.420*	*0.350*	*0.290*

[a] Multi-stage flashing.
[b] Multi-effect distillate.
[c] Seawater reverse osmosis.

Several studies were reported on the direct-contact spray evaporation and condensation (DCSEC) system. In 1981, Miyatake et al [12,13] conducted experiments on spray flash evaporation within a superheated water jet pumped through a nozzle into a low-pressure chamber, where the feed temperatures were varied from 40 °C to 80 °C. From their experiments, empirical equations were developed for the prediction of distillate production. In 2005, Muthunayagam et al [14] evaluated the flash evaporation performance by both numerical and experimental methods on saline water at low feed temperatures, between 26 and 32 K at vacuum pressures less than 2.40 kPa. They reported good agreement between predictions and experiments. In 2006, Ikegami et al [15] compared experiments between opposite directions of injection, i.e., upward and downward jets on the performance of spray flash desalination, at assorted liquid superheat (24–40 K) and feed temperatures from a low-pressure vapor zone. They observed that the flash evaporation process performed better and yet with a shorter distance in an upward direction. Following 2009 and 2010, Mutair and Ikegami [16,17] conducted similar studies of flash evaporation using upward jets but with larger nozzles. They found that the intensity of flash evaporation increased with higher initial water temperatures and the degree superheat. El-Fiqi et al [18] presented a flashing process using tap water, at assorted flow rates with the feed temperatures ranging from 40 °C to 70 °C, and the injection pressure up to 6 bar and the degree of superheat ranging from 6 to 18 K. They opined that the chamber length is inversely proportional to water vapor production and flashing efficiency. Recently Chen et al [19] also simulated the droplet evaporation processes in a single-stage configuration and they observed the relationship between increasing water productivity with initial droplet velocity. They highlighted that smaller droplets of feed are important parameters for enhancing the evaporation processes. In a subsequent paper, Chen et al [20] conducted a simulation study on multi-stages direct contact spray evaporation and condensation system. The water production and thermal efficiency for multi-stages were observed significant improvement as compared with a single-stage system. This system has an improved performance ratio, defined as the ratio of the equivalent heat of distillate to heat input, of 6.5 for a 14-stage desalination plant. Wellmann et al [21,22] simulated also a multi-stage low-temperature desalination system powered with 10 $MW_{thermal}$ CSP (concentrated solar power) plant and 7 $MW_{electric}$ diesel engines. The cogeneration plant was predicted to produce 520 m^3 per day of freshwater.

From the above literature review, the important parameters that govern the direct contact spray evaporation and condensation method (DCSEC) of seawater desalination are the necessity for an optimal design of (i) temperature difference between the temperature of feed

Table 3
The design dimensions of key components for DCSEC pilot.

Parameter	Evaporator chamber	Condenser chamber	Side chamber for micro/nano-bubbles generator
Height (mm)	*700*	*700*	*350*
Inter Diameter (mm)	*64*	*64*	*250*
Nozzle distributor	*spray nozzle P-series*	*spray nozzle P-series* [23]	–
link pipe between evaporator and condenser	*Diameter = 100* mm *Length = 100* mm *Flange = NW 100*	*Diameter = 100* mm *Length = 100* mm *Flange = NW 100*	–

All connecting pipes for feed water (evaporator) and potable water (condenser) are 25 mm, stainless steel (316 L) pipes.
All flanges used in the apparatus are either KF16 or KF25.

water and the evaporative chamber, (ii) the feed of seawater to the evaporators and the freshwater to the condensers (iii) the size of water droplets for flashing processes. However, all flashing rates reported in the literature were relatively low with respect to the feed flow rate. In this connection, we propose the incorporation of sub-cool vapor in the form of micro/nano-bubbles into the feed so as to increase the surface area for heat transfer. Thus, the flashing heat transfer rates are improved overcoming the flashing temperature limitations. The details of experimentation are presented in the sections to follow.

2. Experiments

A lab-scale direct-contact spray-assisted evaporation and condensation (DCSEC) desalination system was designed, fabricated, and installed at laboratory LFO 155 of King Abdullah University of Science and Technology (KAUST). It comprises three major components, namely, evaporator and condenser chambers, as well as other supporting external components such as the heater, pumps, heat exchanger, and distillate tank. Table 3 summarizes the design dimensions of key DCSEC components, and the detailed operational parameters employed for the experiments to be conducted are shown in Table 4.

Fig. 1 shows the hollow chambers of evaporator and condenser, interlinked by vapor pipe. Emanating from the side chamber, the feed pump draws seawater into the spray pipe and nozzles of the evaporator and the state of feed water are monitored by flow, pressure and temperature sensors before entering the evaporator. The seawater feed is also preheated externally before being injected through a nozzle. The hollow evaporator chamber is controlled to a temperature lower than the feed water, giving a liquid superheat that promotes liquid flashing. The function of the nozzle is to generate macro-size droplets, typically 0.2 to 0.6 mm in diameters. The phenomenon of liquid flashing is caused by the excess enthalpy embedded within these droplets. Vaporization occurs instantly from the droplet surfaces over milliseconds. The produced vapor from the evaporator moved to the adjacent condenser chamber due to a small pressure difference induced by the condensation of vapor. This phenomenon of condensation is achieved by similar spraying of potable water droplets which is set at a lower temperature as compared to the saturation temperature.

The water production is measured by overflowing of distillate into a collection tank which weighs the distillate over a period. Fig. 2a and b present the pictorial views of the experimental test facility.

The temperatures of feed water, cooling water, hot water, the temperature of chambers, and distilled water were measured by thermistor probes (OMIGA TH-10-44031-120) with ± 0.1 °C accuracy. Feed flow and cooling water flow rates were measured with flowmeters (Aichi Tokei Denki ND20-PATAAA-RC) with ± 2 accuracy. The vacuum pressures in the chambers were measured with pressure sensors of ± 0.03% of span (YOKOGAWA FP201A-L33), as shown instrumentation in Fig. 3.

Table 4
List of parameters adopted for the experiments.

Operation Parameters	Conventional DCSEC	Hybrid DCSEC With MB-generator
Feed temperature range (°C)	38–60	38–60
Cooling temperature range (°C)	35	35
Feed flow rate (LPM)	6	6
Cooling flow rate (LPM)	6	6
Saturation pressure (kPa)	6.62–19.92	6.62–19.92

2.1. Micro/Nanobubbles (M/NB) generator

Despite being sprayed into small droplets of seawater and the excess enthalpy in the droplets, the rate of liquid flashing within the evaporator is still relatively low, as reported from the literature. In this research, we introduced the concept of micro/nano-bubbles to overcome the limitation of low flashing. The distillate production by flashing can be elucidated by the released of excess enthalpy from the surface of brine droplet to vapor of evaporator, that is;

$$\dot{m}_{v,flash} \propto (A_{droplet},\ T_f,\ T_v,\ \dot{m}_f,\ h_{fg}) \tag{1}$$

where T_f, $T_v$are the temperatures of feed and saturation vapor of evaporator. The proportional constant is given by the mass transfer coefficienth_m. Considering the different heat transfer rates for both the conventional liquid droplet and the micro/nano-bubble embedded droplet, the energy balance at any time instance, *t*, is given as below:

$$\dot{Q}_{withoutMB} = h_m \times A_D \times (T_f - T_v)_D = \dot{m}_{withoutMB} \times h_{fg} \tag{2}$$

$$\dot{Q}_{withMB} = h_m \times A_{MB} \times (T_f - T_v)_{MB} = \dot{m}_{withMB} \times h_{fg} \tag{3}$$

where $h_m$refers to mass transfer coefficient, A_D and A_{MB} are the surface areas of a droplet and a droplet with micro/nano-bubbles. Re-arranging the temperature differences ratio in equations (2) and (3) and n is the number of bubbles inside a droplet, the role of micro/nano-bubbles is reflected by their presence as indicated by the term $\left(1 + \frac{nA_{MB}}{A_D}\right) \gg 1$;

$$\frac{\left(1 + \frac{nA_{MB}}{A_D}\right) \times (T_f - T_v)_{MB}}{(T_f - T_v)_D} = \frac{\dot{m}_{withMB}}{\dot{m}_{withoutMB}} \tag{4}$$

From Eq. (4), all parameters can be determined by experimental measurements except the number of micro-bubbles, n. Depending on the diameter size of liquid droplets, typically from 100 to 150 μm, the expected values of n of micro-bubbles vary from 60 to 130.

Fig. 4 shows a simple micro/nano-bubbles device comprising a short circular section of a nominal diameter d_1; On one end is a conical section tapering from d_1 to d_2 and on the other end, the vapor inlet tube d_3 is attached to the core of circular section, whilst the working fluid is injected through an opening d_4 tangentially at 2 bar. The tangential entry of rotating water creates a vortex greater than 1000 rpm, generating a low pressure at the vortex core. It induces the vapor to move from its inlet to the cone outlet, increasing in static pressure along the path. The vapor-water mixture emerges from the mouth (d_2) of the cone section. At the vortex cone outlet, the mixture is slammed against a pool of stagnant water in the side chamber. Owing to the high rotation speed of the mixture, a shearing effect occurs between them, generating

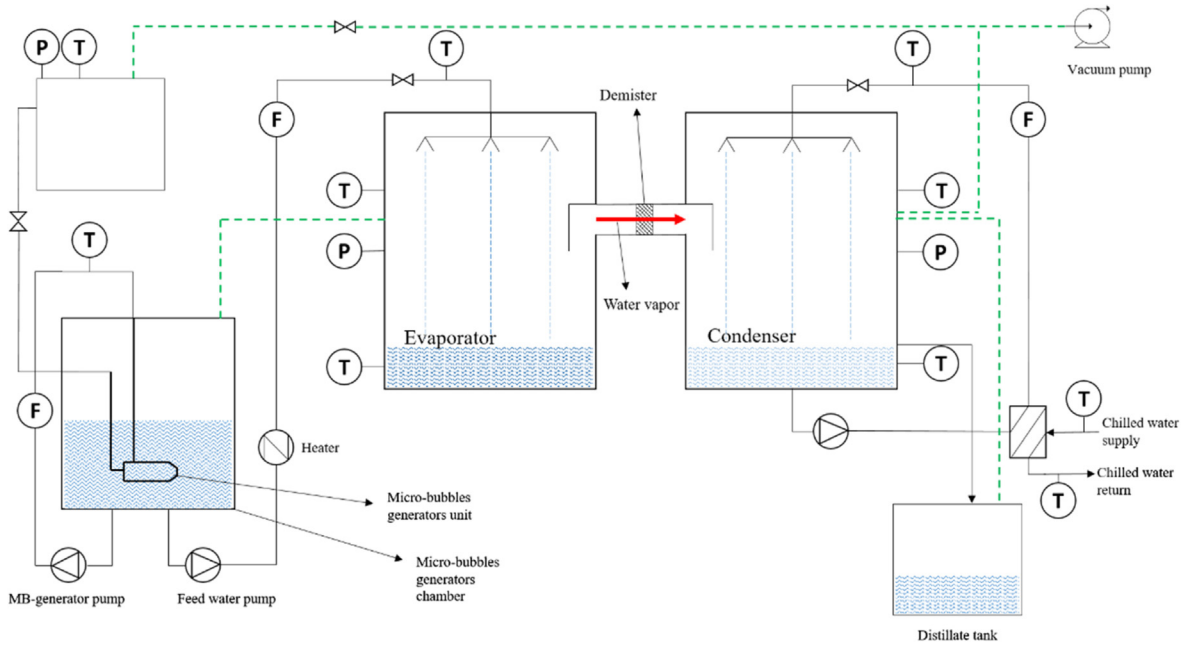

Fig. 1. A schematic diagram of direct contact spray-assisted evaporation (DCSEC) experiment. The symbols F,T and P refer to flow rate, temperature and pressure sensors, respectively.

micro/nano-bubbles in the feed stream to the evaporator chamber. As can be seen from Fig. 2(a), the micro/nano-bubbles device in the experiments is designed as a side injection equipment, supplementing the feed to the evaporator. The injected micro/nano-bubbles are embedded in the feed before spraying into the chamber. As a low pressure and flow rate (6 LPM) pump is used in the micro/nano-bubbles device, the pumping power is insignificant, typically less than 35 W and it constitutes merely 1–2% of heat input to the feed.

2.2. Multi-stages design for DCSEC

Although Fig. 2(a) shows a single-stage design, the experimental setup can also be operated in a multi-stage configuration. To perform the multi-stage operation, a piece-wise technique is adopted here:- The outlet brine temperature of the proceeding stage is set as the feed temperature of subsequent stage and this process is repeated until the outlet brine temperature approaches the ambient conditions (as indicated in table insert of Fig. 5). The advantages of a multi-stage design are (i) the recovery of latent condensation heat of condenser to preheat the incoming seawater feed, (ii) increasing water production by

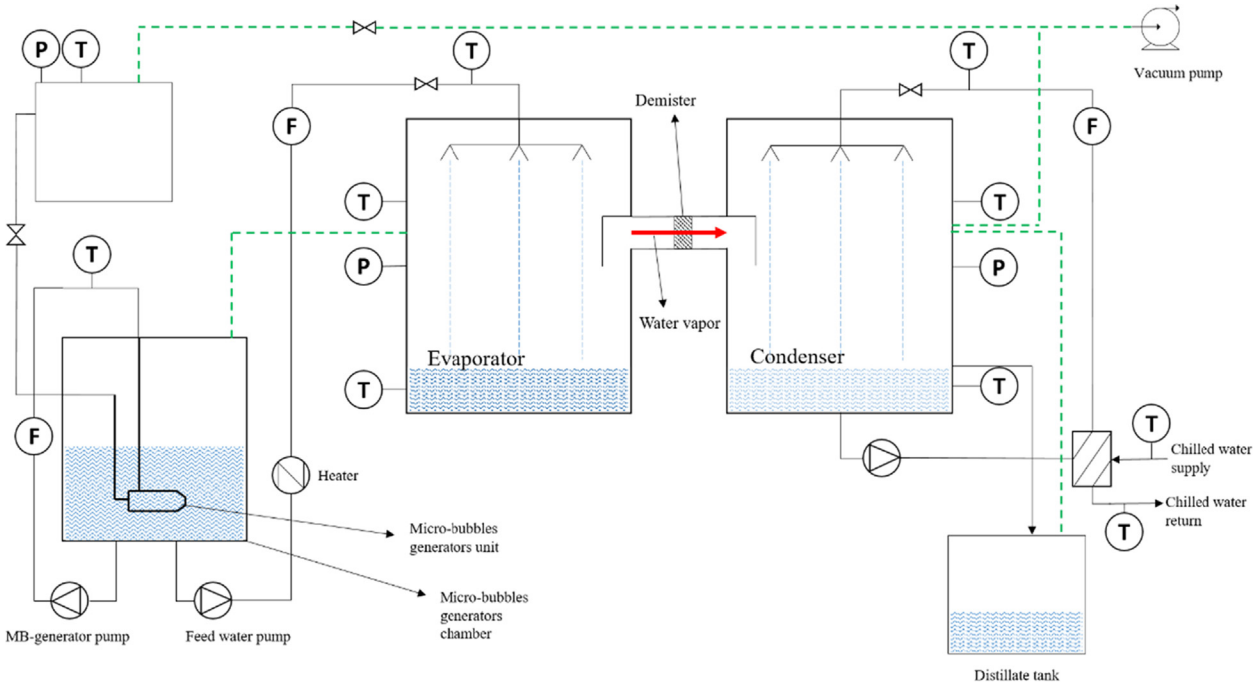

Fig. 2. (a) shows the frontal view of direct contact spray-assisted evaporation (DCSEC) apparatus and (b) shows the side view of the chamber that houses the micro/nano-bubbles generator.

Fig. 2. (*continued*)

Fig. 2. (*continued*)

exploiting more of the excess enthalpy of feed and (iii) high tolerance to increasing brine concentration in succeeding stages due to the favorable temperature gradients.

Fig. 5 shows a typical multi-stage direct contact spray evaporation and condensation (DCSEC) configuration comprising 6- stages of evaporator-condenser pairs, a heat recovery heat exchanger (HX1) to preheat the incoming seawater, a heat source heat exchanger (HX2) to further boost temperature of seawater feed to required entering temperature of top brine stage (TBT) and a vacuum pump to remove any non-condensable gas in the system.

From HX2, the feed water at about 60 °C is fed to the evaporator where the water is distributed above the perforated plate and it flows through the purpose-built holes. Owing to the pressure difference across perforated holes and the hollow chamber of the evaporator, the water jet experiences an accumulation of access enthalpy from the differences in saturation temperatures. Consequently, a fraction of the liquid flashes into vapor to achieve equilibrium. The brine of the stage is fed to the subsequent stage via a U-tube arrangement to overcome the pressure difference. The vapor generated from liquid flashing flows into the adjacent condenser through a connecting pipe where the migrated vapor then condenses onto the cooler surfaces of water droplets that were sprayed through the perforated holes in a similar manner. These processes are repeated in the subsequent stages of the multi-stage design with progressively dropping pressures and temperatures over the stages.

As can be seen from the above sections and also Fig. 5, HX1 preheats the incoming seawater feed from the ambient temperature to the temperature of distillate where the latter collects all latent heat of condensation accumulated by all stages. Concomitantly, HX2 further heat the seawater feed with an external heat source such as the renewable solar or industrial waste heat, etc. The salient feature of multi-stage DCSEC is the opportunity for recovery of the condensation heat up to 70%, while the external heat input needed is 30% of the total heat consumed by the evaporators.

3. Results and discussion:

This section entails the experimental tests of (i) a single-stage direct contact spray evaporation and condensation (DCSEC) with seawater feed varying from 38 °C to 60 °C and (ii) experimentally-emulated multi-stage operation by using the piece-wise technique (described in Section 2.2) starting with a top-brine temperature (TBT) of 60 °C and the cooling water inlet of 35 °C. The sensitivity study of the evaporator volume saturation effect on flashing is also conducted in Section 3.3.

3.1. Single-stage DCSEC and hybrid DCSEC with micro/nano-bubbles (M/NB)

The experiments were conducted at assorted heat sources and feed water flow rates to investigate the performance of DCSEC system in a single configuration operating with and without M/NB. The experimentally measured results are summarized in Table 5. It shows the comparison between distillate production for simple and hybrid DCSEC with and without M/NB generator. The data are expressed in l/hr m^3 where the volume (m^3) refers to the volume of the evaporator vessel. The latter is used as a design parameter of DCSEC as the vessel used is devoid of the physical interface such as the heat transfer tube or membrane area. The figure of merit for distillate production at each feed temperature, termed as the performance ratio (PR) is defined as the ratio of equivalent heat of distillate to input energy from the feed. It is observed the distillate production for the simple DCSEC increases linearly with increasing feed temperature with a gradient of 1.43 L/hr m^3 per degree. However, the hybrid DCSEC with M/NB generator surges with a higher gradient of 2.01 L/hr m^3 per degree over the same temperature range. In terms of the performance ratio, the conventional DCSEC has PR values increasing from 0.50 to 0.75. Nevertheless, the hybrid DCSEC with M/NB_s generator achieved correspondingly higher PR values from 0.55 to 0.91, and the improvement in distillate production is up to 34% comparatively.

3.2. Multi-Stage DCSEC (without micro/nano-bubbles) and hybrid DCSEC with micro/nano-bubbles injection.

In the multi-stage configuration using a piece-wise emulation technique, the outlet brine temperature of the preceding evaporator stage is set as the feed temperature of the following stage. This process is repeated for four to six stages configurations until the bottom outlet brine temperature approaches the ambient temperature. This

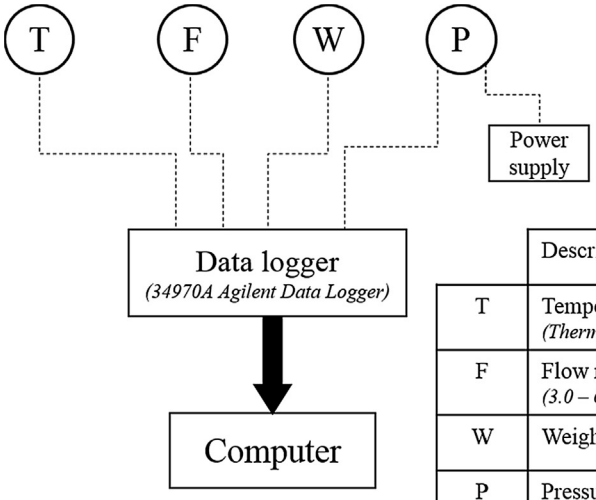

	Description
T	Temperature sensor *(Thermistors, SUS sheath, 10000 ohms, ±0.1C)*
F	Flow meter *(3.0 – 60 L/min, ±2%RS accuracy, 25 mL/P)*
W	Weighing machine
P	Pressure sensor *(0 to 100 kPa abs, 4 to 20 mA DC 2 wire type)*

Fig. 3. Layout of instrumentation for DCSEC pilot facility.

configuration boosts the recovery of latent condensation heat in the condenser to preheat the incoming seawater feed with a heat exchanger. Consequently, the overall distillate production of multi-stage DCSEC increased, as shown in Fig. 6. It can be observed from the figure that the distillate production increases asymptotically with the number of stages, and higher distillate production is found when micro/nano-bubbles were introduced. Correspondingly, the temperature difference between the feed and brine is found to be decreasing inversely manner, i.e., from 5 K to 3.6 K with respect to an increasing number of stages (4–6 stages). From the literature, the flashing phenomenon between liquid droplets and vapor chamber is limited to 3°Kelvin [24,25]. This minimum threshold for flashing is controlled by the non-equilibrium phenomena between the liquid and vapor phase (about 1.5–2 K) and the boiling point evaluation effect (about 1 K) from the salinity of seawater. Consequently, the experiments for multi-stage were limited to six stages as seen in Fig. 6.

Fig. 7 shows the increasing exponential trend of performance ratio (PR) with the number of stages. The increase in PR with an increasing number of stages is attributed to higher distillate production and heat recovery of latent heat condensation from condensers. It is also observed that the presence M/NB in the feed caused a quantum jump of PR due to the increase the surface area of droplets for heat transfer, i.e., the extraction of excess liquid enthalpy to aid flashing phenomena. In addition, the leveling of PR can be attributed to diminishing excess enthalpy as it approaches six or more stages. As compared with the existing thermally-driven methods, namely MSF and MED of six-stages, the performance ratio of DCSEC is comparable to each other at PR equal to 3.30. However, the DCSEC method has the advantage of lower CAPEX because the design of the chamber is devoid of tubes, and secondly, it can handle feed seawater of salinity up to 200 ppt.

3.3. *ume saturation effect for flashing*

The saturation effect of evaporator volume on distillate production

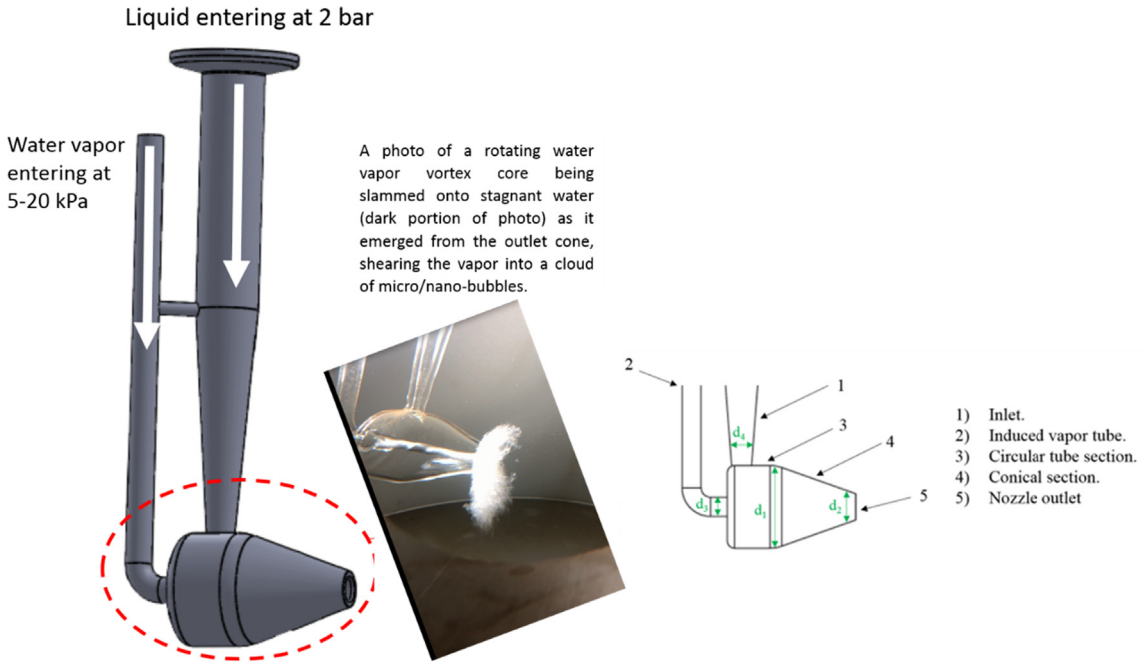

Fig. 4. Schematic diagram of the microbubbles generator device.

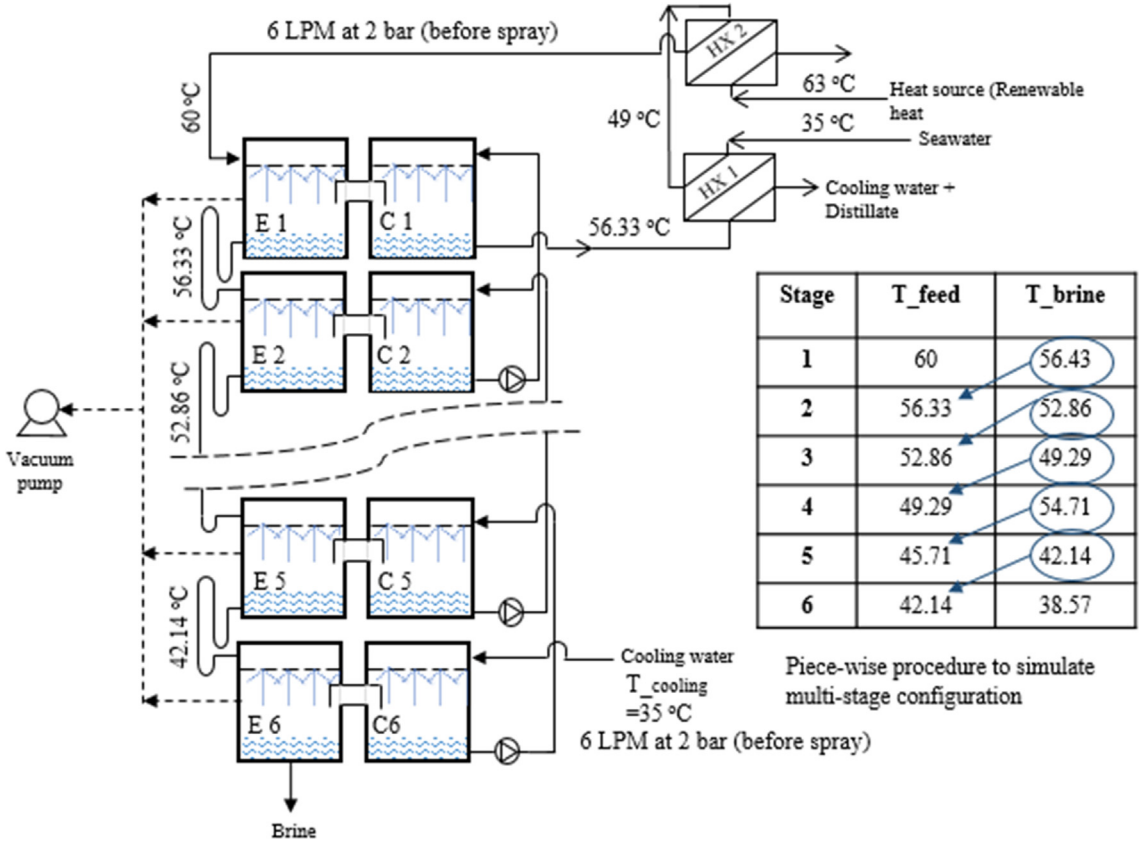

Stage	T_feed	T_brine
1	60	56.43
2	56.33	52.86
3	52.86	49.29
4	49.29	54.71
5	45.71	42.14
6	42.14	38.57

Fig. 5. A schematic diagram demonstrating the multi-stage configuration of a direct contact spray-assisted evaporation and condensation (DCSEC) plant. The table insert shows the piece-wise procedure for a six-stage configuration.

Table 5
Single-stage DCSEC test results with and without micro/nano-bubbles *generator* (M/NB).

Feed temperature (°C)/ saturation absolute pressure (kPa)	Distillate (l/hr.m^{3*} ± 0.01) **volume of evaporator*		Performance Ratio (PR) $=\frac{Distillate\ \ production \times h_{fg}(T_{set}=42^{\circ}C)}{feed\ \ flow\ \ rate \times Cp \times \Delta T}$	
	conventional DCSEC (without M/NB)	Hybrid DCSEC with M/NB generator	conventional DCSEC (without M/NB)	Hybrid DCSEC with M/NB generator
38/ 6.62	3.47	4.07	0.50	0.55
41/7.79	7.48	9.09	0.58	0.68
44/9.10	10.89	14.6	0.63	0.79
47/10.63	15.31	20.88	0.68	0.81
50/12.33	20.74	28.34	0.72	0.84
53/14.38	25.69	35.15	0.74	0.86
56/16.58	30.01	41.08	0.75	0.89
60/19.92	33.44	45.77	0.75	0.91

is important from the viewpoint of designing a DCSEC. For the present analysis, the experimental apparatus is the same in Table 3. However, the feed flow rate is adjusted from 4 LPM to 10 LPM to investigate the distillate production, as shown in Fig. 8. For a given feed temperature, the trend of distillate production is increasing with feed flow rate up to 8 LPM, and it saturates or leveling off afterward. Such a saturation phenomenon can be attributed to the coalesced droplets in the evaporator, probably reducing the surface area for flashing, and hence showing an asymptotic behavior.

4. Conclusion:

We have extensively studied the single and multi-stage direct-contact spray evaporation and condensation (DCSEC) desalination utilizing low feed temperature varying from 38 °C up to 60 °C. It exploits the excess enthalpy of liquid droplets that were sprayed into the evaporator chambers. The flashing phenomenon was further enhanced by introducing sub-cooled micro/nano-bubbles into seawater feed prior to its injection into the evaporator chamber. Such a hybrid DCSEC configuration showed a quantum improvement in the distillate production, up to 34% vis-à-vis over the simple design. The performance ratios (PR) of simple DCSEC configuration increased from 2.71 to 3.53 with the hybrid design using micro/nanobubbles. The low temperature of feed for DCSEC, typically less than 65 °C, can readily be supplied from the renewable solar or industrial waste heat. Being devoid of any physical interface such as membranes or heat exchange tubes, no chemicals are needed to pre-treat the seawater feed. Hence, DCSEC has a low operating cost (OPEX). These salient advantages of DCSEC positioned it to be one of the greener and cost-effective sustainable desalination methods.

Declaration of Competing Interest

The authors declare that they have no known competing financial interests or personal relationships that could have appeared to influence the work reported in this paper.

Acknowledgment

The authors wish to thank the King Abdullah University of Science & Technology (KAUST) (URF/1/2986-01-01), and Aljouf University (JU).

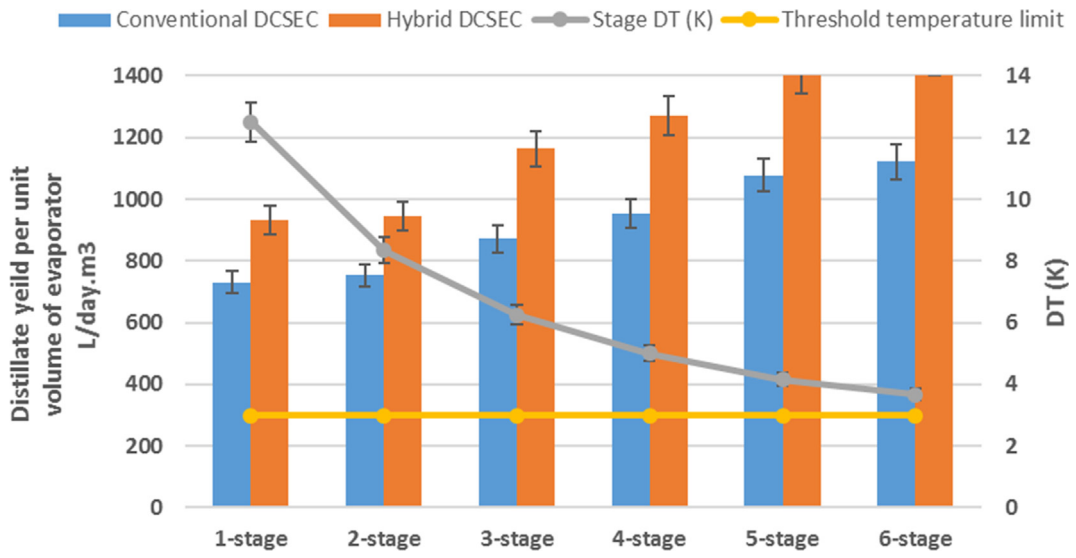

Fig. 6. Distillate production for multi-stage configurations varying from two to six stages. The blue and the brown bars depict the distillate production (L/day.m^3) of conventional (without M/NB) & hybrid DCSEC (with M/NB generator) respectively. The gray (actual DT) and orange (threshold DT limit) lines show the temperature difference between feed and brine in the evaporator chamber at same corresponding configurations. (For interpretation of the references to colour in this figure legend, the reader is referred to the web version of this article.)

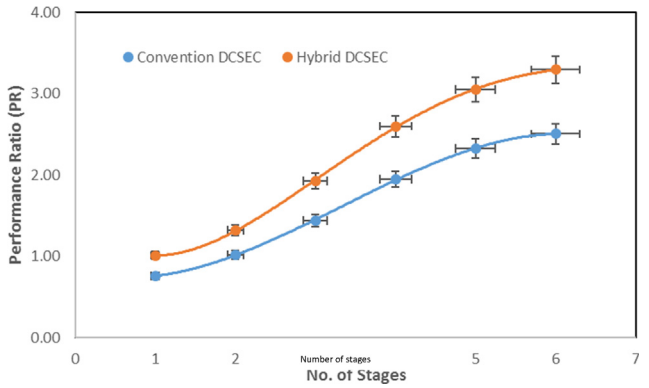

Fig. 7. Performance Ratio (PR) with conventional & hybrid DCSEC with M/NB generator (TBT = 60 °C).

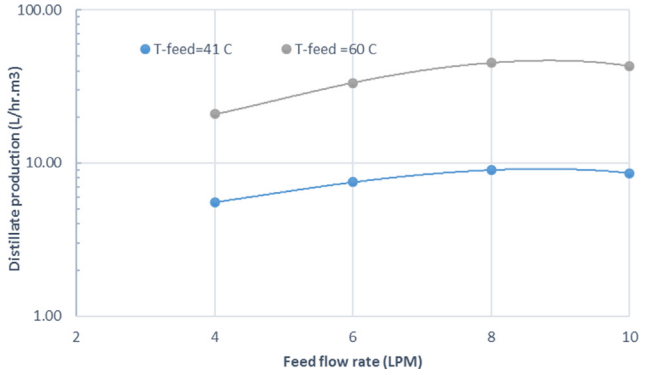

Fig. 8. Sensitivity of distillate production versus feed flow rate at constant evaporator volume.

References

[1] http://www.escwa.un.org/popin/members/saudi%20arabia.pdf (date of access 02-10- 2020).

[2] https://pai.org/wp-content/uploads/2012/04/PAI-1293-WATER-4PG.pdf (date of access 02-10- 2020).

[3] M.W. Shahzad, K. Thu, Y.-D. Kim, K.C. Ng, An experimental investigation on MEDAD hybrid desalination cycle, Appl. Energy 148 (2015) 273–281, https://doi.org/10.1016/j.apenergy.2015.03.062.

[4] J. Zhao, M. Temimi, H. Ghedira, Characterization of harmful algal blooms (HABs) in the Arabian Gulf and the Sea of Oman using MERIS fluorescence data, ISPRS J. Photogramm. Remote Sens. 101 (2015) 125–136, https://doi.org/10.1016/j.isprsjprs.2014.12.010.

[5] Maryam R. Al Shehhi, Imen Gherboudj, Hosni Ghedira, An overview of historical harmful algae blooms outbreaks in the Arabian Seas, Mar. Pollut. Bull 86 (1–2) (2014) 314–324. https://doi.org/10.1016/j.marpolbul.2014.06.048.

[6] Lattemann, Sabine, et al., Global desalination situation, Sustain. Sci. Eng. 2 (2010) 7–39. https://doi.org/10.1016/S1871-2711(09)00202-5.

[7] P.M. Glibert, J.H. Landsberg, J.J. Evans, M.A. Al-Sarawi, M. Faraj, M.A. Al-Jarallah, A. Haywood, S. Ibrahem, P. Klesius, C. Powell, C. Shoemaker, A fish kill of massive proportion in Kuwait Bay, Arabian Gulf, 2001: the roles of bacterial disease, harmful algae, and eutrophication, Harmful Algae 1 (2) (2002) 215–231, https://doi.org/10.1016/S1568-9883(02)00013-6.

[8] Loreen O. Villacorte, et al., Algal blooms: an emerging threat to seawater reverse osmosis desalination, Desalin. Water Treat. 55 (10) (2015) 2601–2611. https://doi.org/10.1080/19443994.2014.940649.

[9] K.C. Ng, K. Thu, S.J. Oh, L.i. Ang, M.W. Shahzad, A.B. Ismail, Recent developments in thermally-driven seawater desalination: energy efficiency improvement by hybridization of the MED and AD cycles, Desalination 356 (2015) 255–270, https://doi.org/10.1016/j.desal.2014.10.025.

[10] Muhammad Wakil Shahzad, Muhammad Burhan, Kim Choom Ng, A standard primary energy approach for comparing desalination processes, npj Clean Water 2(1) (2019) 1. https://doi.org/10.1038/s41545-018-0028-4.

[11] Qian Chen, Kian J. Chua, A spray assisted low-temperature desalination technology, Emerging Technologies for Sustainable Desalination Handbook. Butterworth-Heinemann, 2018, 255–284. https://doi.org/10.1016/B978-0-12-815818-0.00008-4.

[12] O. Miyatake, T. Tomimura, Y. Ide, T. Fujii, An experimental study of spray flash evaporation, Desalination 36 (2) (1981) 113–128, https://doi.org/10.1016/S0011-9164(00)88635-X.

[13] O. Miyatake, T. Tomimura, Y. Ide, M. Yuda, T. Fujii, Effect of liquid temperature on spray flash evaporation, Desalination 37 (3) (1981) 351–366, https://doi.org/10.1016/S0011-9164(00)88658-0.

[14] A.E. Muthunayagam, K. Ramamurthi, J. Robert Paden, Modelling and experiments on vaporization of saline water at low temperatures and reduced pressures, Appl. Therm. Eng. 25 (5-6) (2005) 941–952, https://doi.org/10.1016/j.applthermaleng.2004.08.005.

[15] Y. Ikegami, H. Sasaki, T. Gouda, H. Uehara, Experimental study on a spray flash desalination (influence of the direction of injection), Desalination 194 (1) (2006) 81–89, https://doi.org/10.1016/j.desal.2005.10.026.

[16] Sami Mutair, Yasuyuki Ikegami, Experimental investigation on the characteristics of flash evaporation from superheated water jets for desalination, Desalination 251 (1–3) (2010) 103–111, https://doi.org/10.1016/j.desal.2009.09.136.

[17] Sami Mutair, Yasuyuki Ikegami, Experimental study on flash evaporation from superheated water jets: Influencing factors and formulation of correlation, Int. J. Heat Mass Transf. 52 (23–24) (2009) 5643–5651, https://doi.org/10.1016/j.ijheatmasstransfer.2009.05.009.

[18] Adel K. El-Fiqi, et al., Flash evaporation in a superheated water liquid jet, Desalination 206 (1–3) (2007) 311–321, https://doi.org/10.1016/j.desal.2006.05.017.

[19] Q. Chen, et al., Development of a model for spray evaporation based on droplet

analysis, Desalination 399 (2016) 69–77, https://doi.org/10.1016/j.desal.2016.08.017.
[20] Q. Chen, Y. Li, K.J. Chua, On the thermodynamic analysis of a novel low-grade heat driven desalination system, Energy Convers. Manage. 128 (2016) 145–159, https://doi.org/10.1016/j.enconman.2016.09.070.
[21] Johannes Wellmann, et al., Modeling an innovative low-temperature desalination system with integrated cogeneration in a concentrating solar power plant,: Desalin. Water Treat. 55 (12) (2015) 3163–3171. https://doi.org/10.1080/19443994.2014.940212.
[22] Johannes Wellmann, Bernhild Meyer-Kahlen, Tatiana Morosuk, Exergoeconomic evaluation of a CSP plant in combination with a desalination unit, Renewable Energy 128 (2018) 586–602, https://doi.org/10.1016/j.renene.2017.11.070.
[23] http://www.wilsonspraynozzle.sg/ nozzles model number P66, (date of access 02-10- 2020).
[24] Haoyu Wu, et al., Influence of initial temperature on flashing evaporation, in: IOP Conference Series: Materials Science and Engineering, vol. 381. No. 1. IOP Publishing, 2018. https://doi.org/10.1088/1757-899X/381/1/012125.
[25] Osamu Miyatake, Toshiyuki Hashimoto, Noam Lior, The relationship between flow pattern and thermal non-equilibrium in the multi-stage flash evaporation process, Desalination 91 (1) (1993) 51–64, https://doi.org/10.1016/0011-9164(93)80046-P.